Electron bow-wave injection of electrons in laser-driven bubble acceleration

Y. Y. Ma,[1,2,3,*] S. Kawata,[2] T. P. Yu,[1,4] Y. Q. Gu,[2] Z. M. Sheng,[5] M. Y. Yu,[6,7] H. B. Zhuo,[1] H. J. Liu,[2] Y. Yin,[1] K. Takahashi,[2] X. Y. Xie,[1] J. X. Liu,[1] C. L. Tian,[1] and F. Q. Shao[1]

[1]*College of Science, National University of Defense Technology, Changsha 410073, China*

[2]*Center for Optical Research and Education, Graduate School of Engineering, Utsunomiya University, 7-1-2 Yohtoh, Utsunomiya 321-8585, Japan*

[3]*Laser Fusion Research Center, China Academy of Engineering Physics, Mianyang 621000, China*

[4]*Institut für Theoretische Physik I, Heinrich-Heine-Universität Düsseldorf, 40225 Düsseldorf, Germany*

[5]*Department of Physics, Shanghai Jiao Tong University, Shanghai 200240, China*

[6]*Institute for Fusion Theory and Simulation, Department of Physics, Zhejiang University, Hangzhou 310027, China*

[7]*Theoretical Physics I, Ruhr University, D-44801 Bochum, Germany*

(Received 5 October 2011; published 3 April 2012)

An electron injection regime in laser wake-field acceleration, namely electron bow-wave injection, is investigated by two- and three-dimensional particle-in-cell simulation as well as analytical model. In this regime electrons in the intense electron bow wave behind the first bubble catch up with the bubble tail and are trapped by the bubble finally, resulting in considerable enhancement of the total trapped electron number. For example, with the increase of the laser intensity from 2×10^{19} to 1×10^{20} W/cm^2, the electron trapping changes from normal self-injection to bow-wave injection and the trapped electron number is enhanced by two orders of magnitude. An analytical model is proposed to explain the numerical observation.

DOI: 10.1103/PhysRevE.85.046403 PACS number(s): 52.38.Kd, 41.75.Jv, 52.65.Rr

I. INTRODUCTION

Much progress has been made in laser particle acceleration. In particular, nearly monoenergetic short bunches of energetic electrons have been produced by laser wake-field acceleration (LWFA) [1–4], with which a short-pulse laser-driven large-amplitude fast wake plasma wave traps some of the plasma electrons and accelerates them to relativistic energy. For most applications, such as ion acceleration [5,6], fast ignition in inertial fusion [7], and generation of attosecond electron pulses [8,9], γ rays [10], x rays [11,12], and THz radiation [13,14], the total charge of the energetic electron bunch is important. However, since the total number of accelerated electrons in the LWFA is in general rather small, efficient injection of additional electrons into the acceleration region is necessary. Many optical and plasma-related electron injection techniques have been proposed and demonstrated [15–18]. These include ponderomotive injection [19], colliding-pulses injection [20–22], density-transition injection [23,24], local ionization of neutral atoms [25–27], etc. However, normal self-injection (NSI) of the ponderomotively expelled electrons at the bubble tail remains the basic injection mechanism [1–4]. Several theoretical models have been proposed, and the conditions for self-injection obtained [28,29]. However, more effective injection and acceleration of a large number of electrons are still needed.

In the bubble [30] or blowout [31] regime of LWFA, plasma electrons in the path of the laser pulse are expelled by the laser ponderomotive force, generating a wake bubble that is bounded by a thin enhanced-density electron sheath layer. During intermittent wave breakings a small fraction of the sheath electrons can be self-injected into the tail part of the bubble and accelerated forward by the intense space-charge field there. Most of the sheath electrons remain outside the bubble [19]. Electron bow waves (EBWs) are often also excited at the front, along the periphery of, as well as behind, the bubble [32]. EBWs excited at the front of the bubble were reported by Esirkepov [32]. As expected, the front and side EBWs do not contribute much to the bubble trapped electrons.

II. ELECTRON BOW WAVE INJECTION AND SIMULATION

Here we consider another electron injection regime. As illustrated in Fig. 1, a high-intensity laser pulse enters the plasma from the vacuum and pushes the local electrons away, producing an open cavity bounded by an electron-rich sheath. Simultaneously, two groups of electrons, also at enhanced density (indicated by two small circles on the vacuum-plasma boundary in Fig. 1), are formed on both sides of the cavity, which eventually closes to form a bubble as the laser pulse moves forward into the plasma. The two groups of electrons on the sides meet at the bubble tail, forming a single fast EBW, which propagates forward behind the bubble. The electrons at the center (i.e., on the laser-axis line) of the EBW can catch up with and enter into the bubble. This efficient EBW injection (EBWI) mechanism relies on an initial configuration with which a relativistically propagating intense EBW containing energetic electrons is formed immediately behind the primary bubble at the time of its completion, such that a large number of electrons from the pristine plasma participate in its dynamics.

To demonstrate the EBWI process, we use the 2D3V particle-in-cell (PIC) code PLASIM [33,34] and the 3D PIC code VLPL [35]. For the two-dimensional (2D) case, the simulation box is $200\lambda_0 \times 100\lambda_0$, where $\lambda_0 = 0.8\,\mu$m is the wavelength of the incident laser in vacuum. The incident laser is given by the normalized laser amplitude $a = a_0 \exp[-(t-t_0)^2/\tau^2 - (y-y_0)^2/\sigma^2]$, where $\tau = 10T$, $\sigma = 6\lambda_0$, and T is the laser period. Its intensity is $I =$

*plasim@163.com

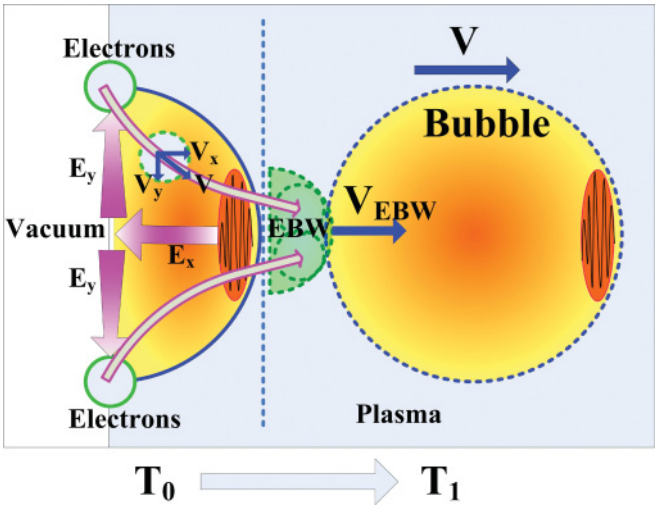

FIG. 1. (Color online) Electron bow-wave (EBW) production. A high intensity laser enters the plasma from vacuum and pushes the local electrons outward. At T_0 an electron sheath in the form of a half bubble is produced. As the laser propagates, the front of the half bubble is extended forward. The enhanced-density sheath electrons at the vacuum-plasma boundary, as marked by the two small (green) circles, are accelerated radially inward as well as axially forward before they meet at T_1. The bubble is then closed; following it is an EBW consisting mainly of the dense electrons from the vacuum-plasma boundary. Injection into the bubble occurs when some of the EBW electrons become faster than the bubble tail.

5×10^{19} W/cm^2, or $a_0 = 4.83$. The laser, linearly polarized in the y direction, enters from the left boundary of the simulation box and propagates along the x axis. The plasma density is $0.002n_c$, or 3.48×10^{18}cm^{-3}, where the critical density is $n_c = 1.74 \times 10^{21}$cm^{-3}. The scale length over which the plasma density rises to its full value is zero here.

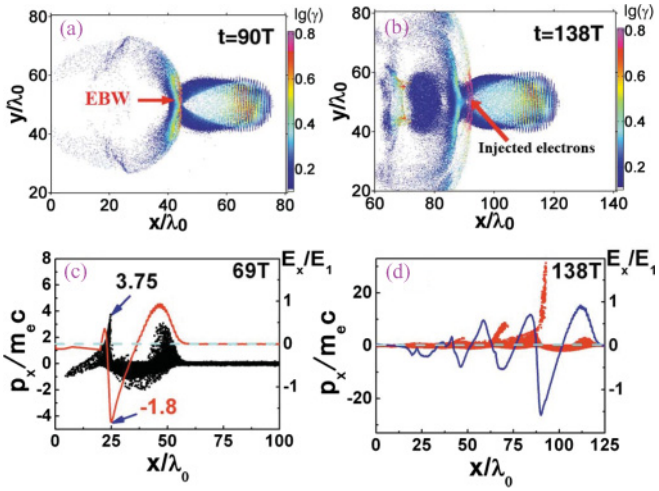

FIG. 2. (Color online) Results for $I = 5 \times 10^{19}$ W/cm^2. Electron energy distributions at $90T$ (a) and $138T$ (b). Electron phase space (dots, left scale) and longitudinal electric field (red and blue curves, right scale) at $69T$ (c) and $138T$ (d).

For appropriate laser intensity and plasma density, a highly nonlinear and highly localized solitonlike EBW with large transverse extent appears behind the primary bubble when its formation is just completed. Figure 2(a) shows that the EBW, consisting of a bowlike layer of electrons at high density, is excited just behind the bubble. The EBW can be considered as a 2D bubble-excited nonlinear solitary electron plasma wave involving a large number of mostly background plasma electrons. The electric field of the EBW in the transverse direction is highly nonuniform near the center, which also moves faster than the rest of the wave. The electric field at the center is so large that it can drive the electrons there into the bubble, as can be seen in Figs. 2(a) and 2(b). In particular, Fig. 2(b) explicitly shows that fast EBW electrons [the "injected electrons" in Fig. 2(b)] can indeed enter into the bubble, and Figs. 2(c) and 2(d) show that many of them are trapped and accelerated to high energy by the longitudinal electric field. We see that the center part of the EBW actually merges with the bubble tail and most of the electrons there can enter the bubble. Together with the EBW electrons, some of the laser-expelled electrons in the bubble boundary are also injected, but their number is much smaller. In contrast, in the NSI regime, only the bubble sheath electrons are injected and the injection depends on the intermittent wave breakings. Furthermore, in the NSI regime electron injection does not start until the laser and the bubble have already propagated several hundred microns into the plasma [28,29,36]. In the EBWI regime, the EBW electrons contribute most to the injected electrons and their injection takes place as soon as the bubble formation is complete. Thus EBWI and NSI are different processes. In particular, in the former most of the bubble-trapped electrons are from the very large and intense EBW consisting of background (instead of laser displaced, like in NSI) plasma electrons.

Figure 3 shows the trajectories of some typical injected and trapped accelerated electrons originally from the EBW. One can clearly see from Fig. 3(a) that they come from a region where the bow wave is first formed, namely near the left plasma boundary, and the results are in good agreement with the principle of the production of EBW in Fig. 1. Figure 3(b) shows the trajectories of two typical injected, trapped, and accelerated electrons originally from the EBW. One can see that after they are trapped in the bubble, they are accelerated and gain more and more energy. As expected, in Fig. 3(b) one

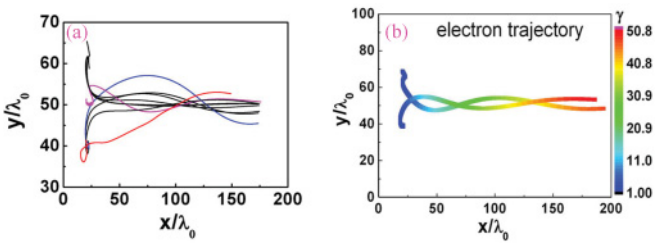

FIG. 3. (Color online) Trajectories of several typical trapped electrons (a). Trajectories and energy gain (color coded) of two trapped and accelerated electrons (b), showing how electrons are trapped and accelerated in the EBW and the bubble.

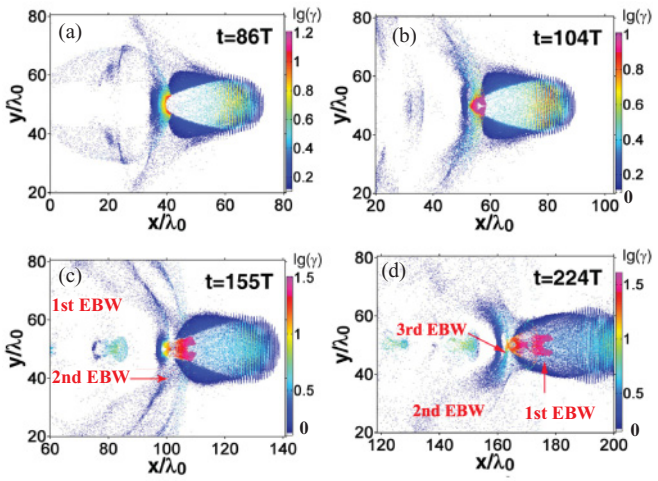

FIG. 4. (Color online) Electron energy distribution for $I = 10^{20}\mathrm{W/cm}^2$ at $86T$ (a), $104T$ (b), $155T$ (c), and $224T$ (d). The EBW electrons catch up with and merge into the elongating tail of the bubble.

can also see that the bubble-trapped electrons exhibit betatron oscillations in the transverse direction [37].

For realizing the EBWI regime, high laser intensity is required to generate a sufficiently nonlinear EBW behind the bubble, so that a large number of energetic electrons can be injected, trapped, and accelerated in order to increase the total charge of the accelerated electron bunch [38]. In fact, the higher the laser intensity, the more intense is the EBW electric field and the more electrons are in the wave and can enter into the bubble. Figure 4 shows the EBWI process for $I = 10^{20}$ W/cm^2, i.e., twice as large as that for Fig. 2. In Fig. 4(a) at $t = 86T$ we can see that the energetic electrons in the first EBW are just behind the bubble. Figure 4(b) at $t = 104T$ shows that the electrons at the center of the EBW have caught up with the bubble tail and entered into it. Figure 4(c) shows that at $t = 155T$ the bubble-trapped electrons originating from the EBW are accelerated. One can also see that a second EBW front has appeared behind the first one. Figure 4(d) shows that at $t = 224T$ the energetic electrons of the second EBW are entering into the bubble. Meanwhile, a third EBW appears. Thus in the entire process a large number of EBW electrons are injected into the bubble. This multiple electron injection process results in a much larger number of trapped and accelerated electrons in the bubble tail than that in the NSI regime. On the other hand, the injected EBW electrons are not well concentrated on the axis like that in NSI. Instead, they occupy a rather large region in the bubble tail. This behavior can be attributed to the interaction of the intense EBW with bubble tail when its center part catches up with the elongating tail of the bubble and merges with it (see Fig. 4) as well as the high charge density of the electron bunch.

The effect of the laser intensity on the number and the maximum energy of the trapped electrons is shown in Figs. 5(a) and 5(b), respectively. We can see that for $I_0 = 2 \times 10^{19}$ W/cm^2 (still in the NSI regime), the number of bubble-trapped electrons increases very slowly as the bubble propagates. On the other hand, for $I_0 = 5 \times 10^{19}$ W/cm^2

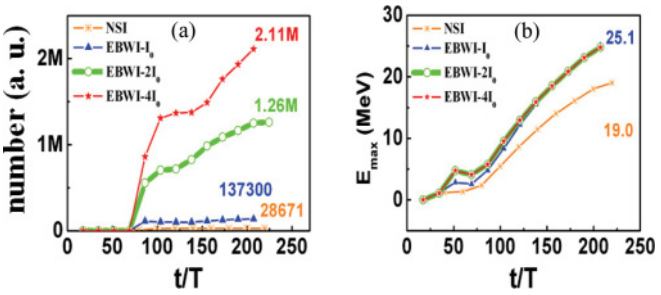

FIG. 5. (Color online) The number of trapped electrons (a), and the maximum energies (b) of trapped electrons for different laser intensity. The numbers in (a) and (b) indicate the maximum electron number and maximum electron energy, respectively, for the corresponding cases.

(weak EBWI regime), the number of bubble-trapped electrons increases rapidly as soon as the bubble is formed. For $I_0 = 1 \times 10^{20}$ W/cm^2 (stronger EBWI regime), the trapped electron number is over nine times that for weak EBWI and about 200 times that for NSI. The trapped electron number can be enhanced further by increasing the laser intensity, but the efficiency decreases. For example, at $I_0 = 2 \times 10^{20}$ W/cm^2, the trapped-electron number is only 1.67 times that for $I_0 = 1 \times 10^{20}$ W/cm^2.

It should be pointed out that the results presented here, such as the maximum injected electron number shown in Fig. 5, has been obtained when there is a rather abrupt density transition between the left vacuum region and the bulk plasma. The effects of the finite transition length at the left vacuum-plasma boundary on the number of the trapped electrons are also studied. It is found that the injected electron number is sensitive to this length. For transition lengths of 5λ, 10λ, and 20λ, the electron bow wave and resulting electron injection can still occur. However, the number of EBWI and thus the bubble trapped electrons tends to decrease with increasing density scale length. The maximum trapped electron number is obtained when the scale length is zero. At $190T$, the trapped electron number is about 85% of the maximum when the scale length is 5λ, and the trapped electron number is only 42% of the maximum when the scale length is 20λ.

We have also conducted 3D PIC simulations of the process using the code VLPL with same laser and plasma parameters.

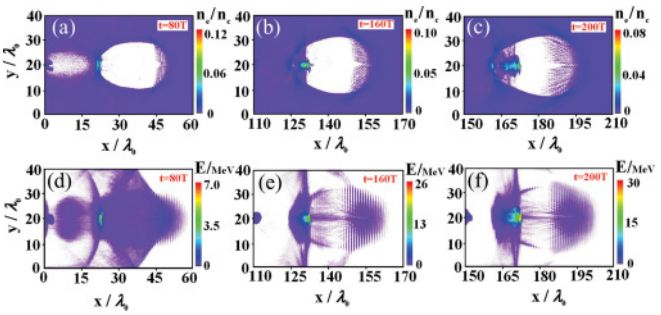

FIG. 6. (Color online) Distributions of the electron density (a)–(c) and energy (d)–(f) at $80T$, $160T$, and $200T$ from 3D PIC simulations using VLPL.

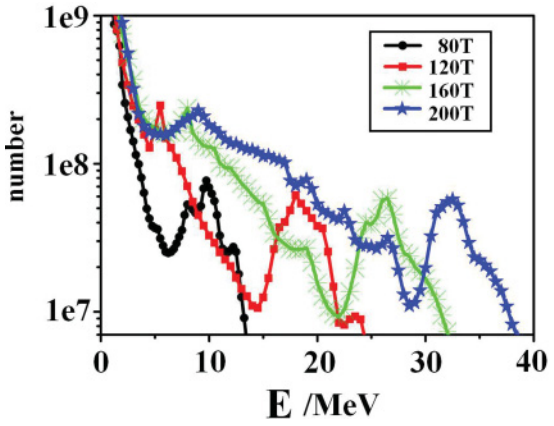

FIG. 7. (Color online) The energy spectra for trapped electrons at $80T$, $120T$, $160T$, and $200T$ from 3D PIC simulations using VLPL.

The EBW and EBWI are also found, as shown in Fig. 6. The total charge of the energetic electron bunch in the bubble is about 0.16 nC, which is of the same order as that obtained from the NSI experiments with a 3-mm-long plasma [3]. The plasma in our simulation is no more than 160 μm. Figure 5 also shows that electron trapping varies nonuniformly with time, which has been also observed in Ref. [28]. The trapped electron number can be controlled by the laser parameters, but the maximum energy of the EBWI electrons remains almost the same for different laser intensities, as shown in Fig. 5(b). It is of interest to note that unlike the bow waves observed and investigated in the existing literature, the EBW of interest here is noticeable only when the electron energy or electron energy density is monitored. In fact, it is not obvious at all in the electron density shown in Figs. 6(a)–6(c). This may be the reason why the EBW considered here has not been noticed in the earlier investigations. The energy spectrum of the trapped electrons at $80T$, $120T$, $160T$, and $200T$ from the 3D PIC simulations are shown in Fig. 7, which shows that the resulting electron bunch is nearly monoenergetic.

III. CONDITIONS FOR EBWI

The conditions for EBWI can be estimated analytically by noticing that first an intense EBW at the back of the bubble should be generated. Second, during its evolution the center of the EBW should propagate faster than the bubble tail. Our simulations indicate that the first condition is actually covered by the second one, which can be expressed as $\gamma_{\rm EBW} > \gamma_{bt}$, where $\gamma_{\rm EBW}$ and γ_{bt} are the relativistic factors of the EBW and the bubble tail, respectively, at the start of EBW formation. The EBW is generated as soon as the bubble tail passes through the left plasma boundary, so that the acceleration length l of trapped electrons should be half the plasma wavelength λ_p. The quantity $\gamma_{\rm EBW}$ can be obtained from the energy balance relation $eE_x l = (\gamma_{\rm EBW} - 1)m_e c^2$, where m_e is the electron mass and c is the speed of light. The profile of the electric field E_x is roughly triangular, so we get $|eE_{x\,\max}|l/2 = (\gamma_{\rm EBW} - 1)m_e c^2$, where $E_{x\,\max}$ has been normalized by $cm_e\omega_p/e$ and l by c/ω_p, with e the electron charge and ω_p the plasma frequency. Replacing l by $\lambda_p/2$, we obtain

$$\gamma_{\rm EBW} = \frac{\pi}{2}|E_{x\,\max}| + 1. \tag{1}$$

From Fig. 2(c) we find that the electron bow wave appears at $69T$ and $E_{x\,\max} = -1.8$. Accordingly, from formula (1) one finds $\gamma_{\rm EBW} = 3.83$, which as agrees well with the maximum value $\gamma = 3.75$ of the EBW electrons at $69T$ in Fig. 2(c). Thus relation (1) is useful for predicting the value of $\gamma_{\rm EBW}$. Moreover, for this case we find $\gamma_{bt} = 3.0$ from the simulation results, so that the condition $\gamma_{\rm EBW} > \gamma_{bt}$ for EBWI to exist is satisfied.

The main differences between NSI and EBWI are as follows: First, the conditions are quite different. The EBWI occurs only for very intense laser pulses. The condition for NSI is much less stringent. Second, the source of the injected electrons is very different. The injected electrons for NSI are from the bubble sheath, and those for EBWI are from the EBW behind the bubble tail. Third, the two injection processes are quite different; NSI is slow and intermittent but EBWI is rapid and strong. Fourth, for NSI there is no intense EBW containing energetic electrons behind the primary bubble. In particular, although for NSI weak bow waves and related structures can be observed in the electron density distribution, they are not observable in the electron energy distribution. Finally, unlike the NSI electrons, the EBWI electrons are spatially widely distributed across the bubble cross section. This is because most of the EBWI electrons are from the high-energy EBW instead of the bubble sheath.

IV. CONCLUSIONS

In conclusion, a different regime, namely EBWI, for electron injection in bubble LWFA is reported. The number of bubble-trapped and accelerated electrons increases with the laser intensity. For the parameters under consideration this number is about 200 times that of the NSI regime, and the charge of the accelerated electron bunch can reach 0.16 nC after the bubble has propagated only 160 μm. A simple analytical model is proposed and the condition for EBWI is obtained. The latter is in good agreement with the simulation results.

ACKNOWLEDGMENTS

This work was supported by the National Natural Science Foundation of China (Grants No. 10976031, No. 11175253, No. 10975121, No. 10935002, and No. 10835003), the Science and Technology Development Foundation of the Chinese Academy of Engineering Physics (Grant No. 2009A00102003), the National Basic Research Program of China (Grant No. 2008CB717806). Y. Y. Ma acknowledges the support of the JSPS and CORE of Utsunomiya University, Japan.

[1] S. P. Mangles, C. D. Murphy, Z. Najmudin, A. G. Thomas, J. L. Collier, A. E. Dangor, E. J. Divall, P. S. Foster, J. G. Gallacher, C. J. Hooker, D. A. Jaroszynski, A. J. Langley, W. B. Mori, P. A. Norreys, F. S. Tsung, R. Viskup, B. R. Walton, and K. Krushelnick, Nature (London) **431**, 535 (2004).

[2] C. G. Geddes, C. Toth, T. J. van, E. Esarey, C. B. Schroeder, D. Bruhwiler, C. Nieter, J. Cary, and W. P. Leemans, Nature (London) **431**, 538 (2004).

[3] J. Faure, Y. Glinec, A. Pukhov, S. Kiselev, S. Gordienko, E. Lefebvre, J. P. Rousseau, F. Burgy, and V. Malka, Nature (London) **431**, 541 (2004).

[4] W. P. Leemans, B. Nagler, A. J. Gonsalves, C. Toth, K. Nakamura, C. G. R. Geddes, E. Esarey, C. B. Schroeder, and S. M. Hooker, Nat. Phys. **2**, 696 (2006).

[5] S. C. Wilks, A. B. Langdon, T. E. Cowan, M. Roth, M. Singh, S. Hatchett, M. H. Key, D. Pennington, A. MacKinnon, and R. A. Snavely, Phys. Plasmas **8**, 542 (2001).

[6] H. Schwoerer, S. Pfotenhauer, O. Jackel, K. U. Amthor, B. Liesfeld, W. Ziegler, R. Sauerbrey, K. W. Ledingham, and T. Esirkepov, Nature (London) **439**, 445 (2006).

[7] M. Tabak, J. Hammer, M. E. Glinsky, W. L. Kruer, S. C. Wilks, J. Woodworth, E. M. Campbell, M. D. Perry, and R. J. Mason, Phys. Plasmas **1**, 1626 (1994).

[8] I. Y. Dodin and N. J. Fisch, Phys. Rev. Lett. **98**, 234801 (2007).

[9] Y. Y. Ma, Z. M. Sheng, Y. T. Li, W. W. Chang, X. H. Yuan, M. Chen, H. C. Wu, J. Zheng, and J. Zhang, Phys. Plasmas **13**, 110702 (2006).

[10] W. P. Leemans, D. Rodgers, P. E. Catravas, C. G. Geddes, G. Fubiani, E. Esarey, B. A. Shadwick, R. Donahue, and A. Smith, Phys. Plasmas **8**, 2510 (2001).

[11] E. Esarey, B. A. Shadwick, P. Catravas, and W. P. Leemans, Phys. Rev. E **65**, 056505 (2002).

[12] A. Rousse, K. T. Phuoc, R. Shah, A. Pukhov, E. Lefebvre, V. Malka, S. Kiselev, F. Burgy, J. P. Rousseau, D. Umstadter, and D. Hulin, Phys. Rev. Lett. **93**, 135005 (2004).

[13] J. van Tilborg, C. B. Schroeder, C. V. Filip, C. Tóth, C. G. R. Geddes, G. Fubiani, R. Huber, R. A. Kaindl, E. Esarey, and W. P. Leemans, Phys. Rev. Lett. **96**, 014801 (2006).

[14] W. P. Leemans, C. G. R. Geddes, J. Faure, C. Tóth, J. van Tilborg, C. B. Schroeder, E. Esarey, G. Fubiani, D. Auerbach, B. Marcelis, M. A. Carnahan, R. A. Kaindl, J. Byrd, and M. C. Martin, Phys. Rev. Lett. **91**, 074802 (2003).

[15] T. Y. Chien, C. L. Chang, C. H. Lee, J. Y. Lin, J. Wang, and S. Y. Chen, Phys. Rev. Lett. **94**, 115003 (2005).

[16] C. G. R. Geddes, K. Nakamura, G. R. Plateau, C. Toth, E. Cormier-Michel, E. Esarey, C. B. Schroeder, J. R. Cary, and W. P. Leemans, Phys. Rev. Lett. **100**, 215004 (2008).

[17] E. Oz, S. Deng, T. Katsouleas, P. Muggli, C. D. Barnes, I. Blumenfeld, F. J. Decker, P. Emma, M. J. Hogan, R. Ischebeck, R. H. Iverson, N. Kirby, P. Krejcik, C. O'Connell, R. H. Siemann, D. Walz, D. Auerbach, C. E. Clayton, C. Huang, D. K. Johnson, C. Joshi, W. Lu, K. A. Marsh, W. B. Mori, and M. Zhou, Phys. Rev. Lett. **98**, 084801 (2007).

[18] J. Faure, C. Rechatin, A. Norlin, A. Lifschitz, Y. Glinec, and V. Malka, Nature (London) **444**, 737 (2006).

[19] D. Umstadter, J. K. Kim, and E. Dodd, Phys. Rev. Lett. **76**, 2073 (1996). English.

[20] E. Esarey, R. F. Hubbard, W. P. Leemans, A. Ting, and P. Sprangle, Phys. Rev. Lett. **79**, 2682 (1997).

[21] P. Zhang, N. Saleh, S. Chen, Z. M. Sheng, and D. Umstadter, Phys. Rev. Lett. **91**, 225001 (2003).

[22] X. Davoine, E. Lefebvre, C. Rechatin, J. Faure, and V. Malka, Phys. Rev. Lett. **102**, 065001 (2009).

[23] S. Bulanov, N. Naumova, F. Pegoraro, and J. Sakai, Phys. Rev. E **58**, R5257 (1998).

[24] H. Suk, N. Barov, J. B. Rosenzweig, and E. Esarey, Phys. Rev. Lett. **86**, 1011 (2001).

[25] M. Chen, Z. M. Sheng, Y. Y. Ma, and J. Zhang, J. Appl. Phys. **99**, 056109 (2006).

[26] C. McGuffey, A. G. R. Thomas, W. Schumaker, T. Matsuoka, V. Chvykov, F. J. Dollar, G. Kalintchenko, V. Yanovsky, A. Maksimchuk, K. Krushelnick, V. Y. Bychenkov, I. V. Glazyrin, and A. V. Karpeev, Phys. Rev. Lett. **104**, 025004 (2010).

[27] A. Pak, K. A. Marsh, S. F. Martins, W. Lu, W. B. Mori, and C. Joshi, Phys. Rev. Lett. **104**, 025003 (2010).

[28] I. Kostyukov, E. Nerush, A. Pukhov, and V. Seredov, Phys. Rev. Lett. **103**, 175003 (2009).

[29] S. Kalmykov, S. A. Yi, V. Khudik, and G. Shvets, Phys. Rev. Lett. **103**, 135004 (2009).

[30] A. Pukhov and J. Meyer-ter-Vehn, Appl. Phys. B **74**, 355 (2002).

[31] J. B. Rosenzweig, B. Breizman, T. Katsouleas, and J. J. Su, Phys. Rev. A **44**, R6189 (1991).

[32] T. Z. Esirkepov, Y. Kato, and S. V. Bulanov, Phys. Rev. Lett. **101**, 265001 (2008).

[33] Y. Y. Ma, W. W. Chang, Y. Yin, Z. W. Yue, L. H. Cao, and D. Q. Liu, Acta Phys. Sinica **49**, 1518 (2000) (in Chinese).

[34] Y. Y. Ma, W. Chang, Y. Yin, L. H. Cao, and Z. W. Yue, Chin. J. Comput. Phys. **19**, 311 (2002) (in Chinese).

[35] I. Kostyukov, A. Pukhov, and S. Kiselev, Phys. Plasmas **11**, 5256 (2004).

[36] B. S. Xie, H. C. Wu, H. Y. Wang, N. Y. Wang, and M. Y. Yu, Phys. Plasmas **14**, 073103 (2007).

[37] K. Németh, B. Shen, Y. Li, H. Shang, R. Crowell, K. C. Harkay, and J. R. Cary, Phys. Rev. Lett. **100**, 095002 (2008).

[38] D. H. Froula, C. E. Clayton, T. Döppner, K. A. Marsh, C. P. J. Barty, L. Divol, R. A. Fonseca, S. H. Glenzer, C. Joshi, W. Lu, S. F. Martins, P. Michel, W. B. Mori, J. P. Palastro, B. B. Pollock, A. Pak, J. E. Ralph, J. S. Ross, C. W. Siders, L. O. Silva, and T. Wang, Phys. Rev. Lett. **103**, 215006 (2009).